

Available online at www.sciencedirect.com**ScienceDirect**

Procedia Manufacturing 13 (2017) 671–678

Procedia
MANUFACTURINGwww.elsevier.com/locate/procedia

Manufacturing Engineering Society International Conference 2017, MESIC 2017, 28-30 June 2017, Vigo (Pontevedra), Spain

Laser Texturing and Dissimilar Material Joining

E. Ukar^{a,*}, F. Liébana^b, M. Andrés^b, I. Marcos^a, A. Lamikiz^a

^aMechanical Engineering Dpt. (UPV/EHU), Pl. Torres Quevedo 1, Bilbao, 48013, Spain

^bTECNALIA Research & Innovation, Parq. Tec. Bizkaia, C/Geldo Ed.700, Zamudio 48160, Spain

Abstract

Laser texturing is a process used to remove material selectively. Metallic parts were processed in order to create a surface texture that enables metal-polymer joining. This kind of dissimilar joining is carried out combining a pressure fixture and heating using a direct diode laser source. In order to reach a good result, it is critical to texture the surface with correct parameters to generate surface features that maximizes the contact between materials and heating enough the materials to soften the polymer but without melting and degrading the material, so, a temperature control system is necessary to get best results. In this work, the texturing capabilities of conventional CW laser source were explored and numerical model was developed in order to simulate and control the process temperature in the joining interface.

© 2017 The Authors. Published by Elsevier B.V.

Peer-review under responsibility of the scientific committee of the Manufacturing Engineering Society International Conference 2017.

Keywords: Laser texturing, dissimilar joining, modelling

1. Introduction

Laser texturing is a process used to remove material selectively. In metal parts, the material must be evaporated during the process. In order to minimize the heat input short and ultra-short pulse laser sources are typically used. Nevertheless, in some applications this is not a critical fact and conventional pulsed laser sources can be used. These applications include dimple generation to reduce friction coefficient [1] or surface texturing to improve

* Corresponding author. Tel.: +34 946014905; fax: +34 946014215.

E-mail address: eneko.ukar@ehu.eus

osseointegration in medical applications [2]. Another application is surface texturing to improve material adhesion in plastic-metal dissimilar joints.

In the automotive industry weight control in body-in-white structures is becoming a critical point in order to reduce weight and meet the actual environmental legislation. Combination of dissimilar materials allows significant weight reduction with optimal mechanical strength in critical areas [3]. One of the most interesting material combinations is aluminum and glass fiber reinforced plastic. Aluminum alloys present relatively high strength and high corrosion resistance, on the other hand, glass fiber reinforced polymers also have high strength-to-weight ratio and are easy to process. Combination of these two materials is interesting for automotive light parts manufacturing but the joint between them is still a critical point that must be addressed. Mechanical fastening [4] and adhesive bonding [5] are conventional methods to joint materials that cannot be welded. Mechanical fastening includes additional elements like rivets or bolts that increase the total weight and induce severe stress concentration, with direct impact on the mechanical properties. For adhesive bonding, the mixture of reactive components has to be spread on the substrates and wait until curing reaction is completed, making these joining process time consuming and unsuitable for massive industrial manufacture. As alternative, a combination of a pressing fixture with local heating by a laser beam allows joining the materials by partial melting of the polymer. In order to reach a solid joint it is necessary to previously prepare or texture the metal substrate. Solutions like surface anodizing are proposed on the literature [6] to improve the result. Anodizing takes from 10 to 30 minutes and needs aluminum part preprocessing. Other alternatives like laser texturing are faster, give similar results and are easy to implement using a conventional fiber laser [7].

In order to reach shear strength values over 25MPa, both, previous texturing and process parameters, must be optimal. With laser surface texturing the contact surface between materials is maximized but, this textured surface must be different depending on wettability and melt flow rate of the polymer. Typically, polymers with low melt flow rate require a texturing with less peak-valley height in comparison with high melt flow rate polymers, which are able to fill narrower features [7]. In the literature peak-valley height between 20 and 10 μ m is considered optimal for dissimilar joining [8]

Another key point in the joining process is the pressure and the temperature in the joining surface. Closed loop temperature control using a pyrometer is one of the best and most reliable ways to adjust the laser power in order to get a constant welding temperature. This control system is widely used in laser hardening process and can be used in dissimilar welding when direct access to joining surface is possible [9]. In metal-polymer laser joining, the laser heats the face opposite to the joint and there is no direct temperature control. On the other hand, depending on the scanning path followed during the heating, the thermal field in the joint interface is different and power cannot be corrected considering only the aluminum sheet thickness. Numerical simulation of thermal field is an alternative, but factors such us, laser energy distribution, the scanning path and material properties must be correctly modeled in order to get a useful tool.

The main target in the present work was to develop a reliable process for metal-plastic direct joints. To get successful joints was necessary to develop correct laser texturing parameters and develop a laser power control system in order to avoid plastic material over-melting or under-melting during the process. In this work, a conventional laser source was used in pulsed mode to modify the surface and prepare it for plastic-metal direct joint. The texturing was developed using a conventional CW laser, which is typically used in laser cutting and joining applications and is considered as unsuitable for laser texturing applications. Finally, a specific close-loop control was developed based on thermal field, which is calculated using own developed thermal model.

2. Laser texturing

The experimental tests were carried out using a 1kW fiber laser from ROFIN in combination with a scan-head from SCANLAB which maximum working space is 120x120mm. The maximum scanning speed of the scan-head is 10,000mm/s. On the other hand, the fiber laser wavelength is 1,060nm and the spot size is 100 μ m in diameter. The laser source can be operated in CW or pulsed mode up to 5kHz. This frequency determines the cycle duration time, not pulse duration. On the other hand, duty cycle parameter, given in percentage, adjusts the percentage of time within the cycle that laser source is switched on. So, the resulting pulse duration is controlled with both, pulse frequency and duty cycle percentage. For laser texturing operations the laser must be operated in pulsed mode. Since pulse duration

is controlled by the switch off and switch on of the pumping, it is necessary to conduct some experiments in order to get the minimum pulse duration that is possible to achieve for steel removal applications.

This preliminary test consisted in several pulses with different duration at maximum power level of 1kW and maximum frequency of 5kHz. The test duration was adjusted to have same energy input in all test. Since frequency was constant at 5kHz, the pulse length was controlled by duty cycle percentage from 4 μ s to 150 μ s. The overall test duration in each case was adjusted to make constant (0.75s) the total time that laser is switched on. Parameters used are summarized in Table 1. The test was performed in AISI D2 tool steel to avoid reflection effects due to material wavelength absorptivity. This test was carried as a preliminary stage to identify the shortest pulse duration that can be used for material removal applications. This threshold value depends only on the source, not on the material, so this pulse duration can be taken as limit value for other materials also.

Table 1. Test parameters for minimum pulse duration characterization

| Duty Cycle [%] | Test time (s) | Pulse (μ s) | Laser On (s) | Laser Off (s) |
|----------------|---------------|------------------|--------------|---------------|
| 75 | 1.0 | 150 | 0.75 | 0.25 |
| 50 | 1.5 | 100 | 0.75 | 0.75 |
| 25 | 3.0 | 50 | 0.75 | 2.25 |
| 10 | 7.5 | 20 | 0.75 | 6.75 |
| 5 | 15.0 | 10 | 0.75 | 14.3 |
| 2 | 37.5 | 4 | 0.75 | 36.75 |

Following Figure 1 shows hole depth achieved in each case. Theoretically, the depth should be similar in all tests since the overall time that source is switched on is constant. From the figure can be concluded that pulses below 100 μ s energy output is dramatically decreased and they cannot be considered effective pulses.

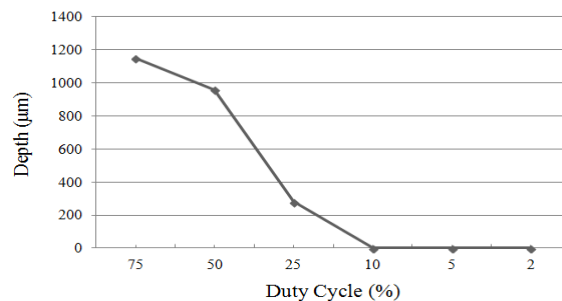


Fig. 1. Reached depth for different pulse duration

Once cleared the minimum pulse duration, an experimental test based on previous data [10] was carried out. The experiments were carried out AISI 304 Stainless steel, which is a widely used material in applications where corrosive resistance is of primary importance. Tested parameters are shown in Table 2. In all tests the scanning speed (feed rate) was adjusted depending on pulse duration to keep as possible constant the beam incidence area in each pulse which is between 0.011 and 0.018mm².

Table 2. Tested parameters

| Parameter | Values |
|------------------|---------------------------------|
| Power [W] | 200 – 250 – 300 – 350 – 400 |
| Frequency [Hz] | 500 – 1000 – 3000 – 4000 – 5000 |
| Feed rate [mm/s] | 300 – 550 – 1000 – 1200 |
| Duty Cycle [%] | 5 – 15 – 20 – 30 – 40 |

The results were evaluated using a Leica DCM 3D confocal profilometer to get 3D topography. The parameters tested provided different results, from dimples with $3\mu\text{m}$ in depth to dimples with $10\mu\text{m}$ depth. To have a proper control of the resulting surface the material removal rate must be highly controlled, so, dimples between 5 and $15\mu\text{m}$ in depth are desirable. The overlapping of dimples allows a controlled texturing. The best results were obtained for pulse duration of $100\mu\text{s}$ with a frequency of 4000Hz , a feed rate of 1000mm/s and a duty cycle of 40% . Figure 2 shows the dimples obtained with theoretical power of 250W and 350W corresponding to energy densities of 0.14kJ/cm^2 and 0.20kJ/cm^2 .

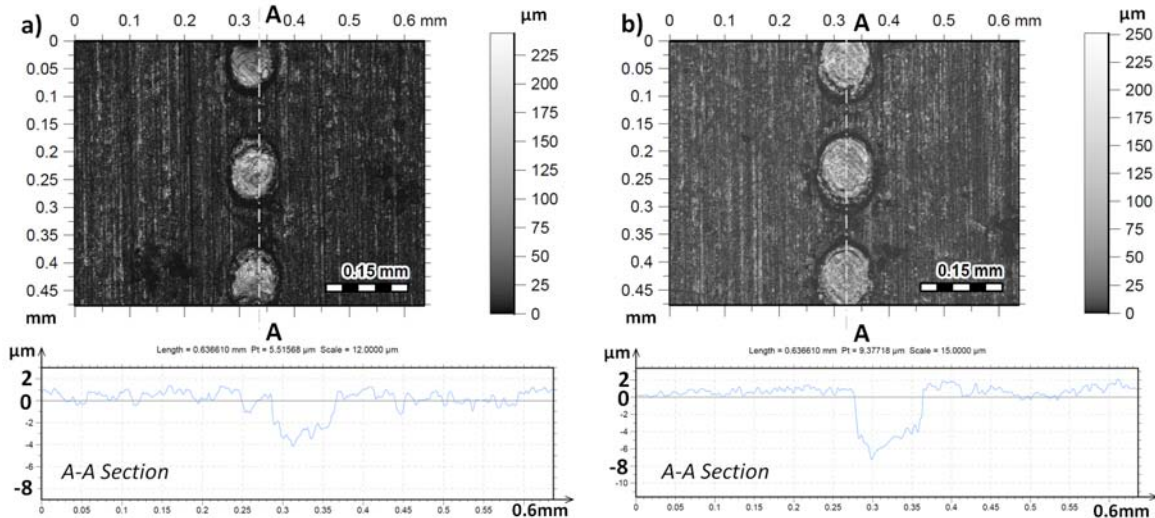


Fig. 2. Single dimples with a) 0.14kJ/cm^2 and b) 0.20kJ/cm^2

In the set-up, the theoretical beam diameter is about $100\mu\text{m}$ and depending on beam power and pulse duration the reached feature diameter is between $50\mu\text{m}$ and $250\mu\text{m}$. When beam power is increased, for longer pulses the resulting feature changes from pin-like shape to a cavity. A fluence over 5kJ/cm^2 and pulse duration of $1000\mu\text{s}$ generates ablation plume and melted material is ejected with no recast. Once reached this situation higher power generates deeper and wider cavities. With most energetic parameters, a cavity of $250\mu\text{m}$ in diameter and $160\mu\text{m}$ in deep was achieved. For $100\mu\text{s}$ pulses the diameter of the resulting surface feature remains below $100\mu\text{m}$ when fluence is below 0.5kJ/cm^2 . With fluence between 0.5 and 1kJ/cm^2 , the material is also removed with less heat affected area and lower penetration, reaching a cavity about $100\mu\text{m}$ in diameter and $50\mu\text{m}$ deep.

With $550\mu\text{s}$ pulses it is also appreciated a transition from pin-like features to cavity formation. The maximum height of pins is also $20\mu\text{m}$, similar to ones reached with $1000\mu\text{s}$ and the cavity shows some under-melted structures because of lack of melting.

For dissimilar joining applications, a high frequency peak-valley distribution is desirable. This surface can be achieved by overlapping low energy pulses and avoiding recast material. In AISI 304 stainless steel best results were obtained with 0.2kJ/cm^2 energy density. In Figure 3, a textured surface of $25\times 12.5\text{mm}^2$ it is show which was scanned four times to reach the final result.

Experiments and the reached result shows that it is possible to get a proper textured surface for dissimilar joining using a CW high power fiber laser. Overlapping dimples is possible to control the depth and roughness level of the resulting surface. In Figure 3 can be appreciated a textured surface with peak-valley height of $15\mu\text{m}$, which is similar to values described in the literature as optimal to get the right texturing for metal-polymer dissimilar joints.

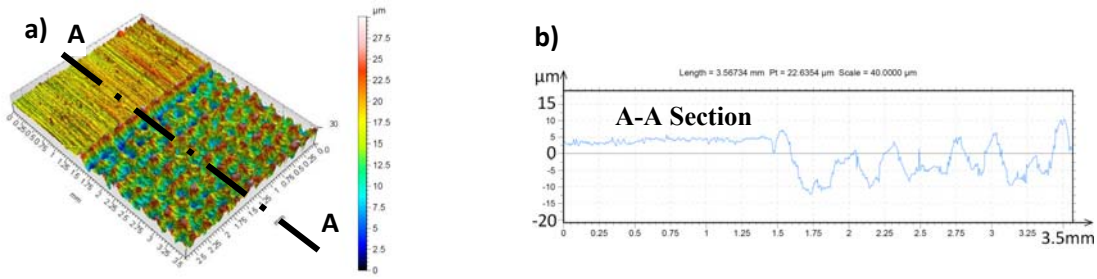


Fig. 3. a) 3D Measurement and b) Extracted profile of laser textured part with 0.2kJ/cm²

3. Thermal field simulation and power control system

To get a satisfactory joint it is necessary to control the temperature of the process carefully to keep it constant during the process. Since it is not possible to have a direct temperature measurement of the joining interface, a numerical model was used to simulate the thermal field and design a control system with 5 different criteria for power management during the process. The model was completely programmed in Matlab[®] starting from basic heat exchange balance shown in Figure 4.

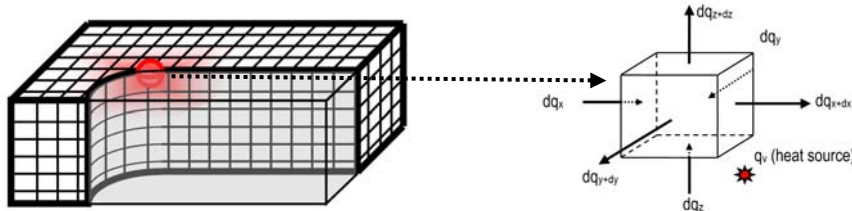


Fig. 4. Heat exchange balance in one element

The thermal model development considers some classical assumptions used on laser material process modelling. The assumptions are:

- Consider the part as a continuous body, homogeneous and isotropic. Thus, the model considers that the heat is transferred in a similar way in all directions.
- Physical properties are constant. Therefore, properties variation with temperature or other parameters are not considered.
- Volume changes due to temperature variations are not considered.

As it has been mentioned, the model is based on the energetic balance for each differential element, as it is shown on Figure 4:

$$dE_{input} - dE_{output} + dE_{generated} = dE_{accumulated} \tag{1}$$

Considering the heat fluxes for each term and each Cartesian direction separately and applying the Taylor series and considering only the independent and first order terms, the following expression is obtained:

$$a \cdot \nabla^2 \theta \pm \frac{q_v}{\rho \cdot c_p} = \frac{\partial \theta}{\partial t} \tag{2}$$

Where a, is thermal diffusivity in m²/s, q_v is the heating power in W/m³, ρ is the density in kg/m³ and C_p is the specific heat in kJ/kg.K. The equation was solved using central-finite-difference method that is easier to program than finite element method and gives accurate result in thermal field simulation [11]. With this method, the differential equation can be written as an explicit expression and therefore solved with a low computational cost. The model was programmed in Matlab[®] following the next expression.

$$T_{x,y,z}^{t+1} = T_{x,y,z}^t + a \cdot \frac{\Delta t}{\Delta x^2} \cdot (T_{x+1,y,z}^t - 2T_{x,y,z}^t + T_{x-1,y,z}^t) + a \cdot \frac{\Delta t}{\Delta y^2} \cdot (T_{x,y+1,z}^t - 2T_{x,y,z}^t + T_{x,y-1,z}^t) + a \cdot \frac{\Delta t}{\Delta z^2} \cdot (T_{x,y,z+1}^t - 2T_{x,y,z}^t + T_{x,y,z-1}^t) \pm \frac{q_v}{\rho \cdot c} \cdot \Delta t \quad (3)$$

Same equation in matrix form can expressed as:

$$\{T^{t+1}\} = [M] \cdot \{T^t\} + \{F\} \quad (4)$$

Finally, contour conditions are introduced: First, the initial condition, $\theta(x,y,z,t=0)=\theta_0$ to set the initial temperature of whole body as θ_0 . Second, set the temperature at the start of one step same as the previous step ending temperature: $\theta(x_s,y_s,z_s,t)=\theta_s$. Finally conserve the same heat flux between two consecutive steps: $q(x_s,y_s,z_s,t)=q_s$. Once calculated the thermal field, is possible to program the temperature control algorithm.

3.1 Temperature control algorithm

The algorithm was programmed in Matlab[®], as a module built into the previous thermal model. The algorithm stabilizes the temperature of the solid in the surrounding area of the operating point by managing the power delivered by the laser at each instant of time. The internal operation of the algorithm is based on five steps. First, the reference temperature "Tref" is set as input parameter. Secondly, the initial temperature of the solid is indicated by a data matrix with the Temperature. The initial one in each of the nodes. Then in the third step, In a first phase of the simulation, specifically, for the first 3 steps of simulation, the algorithm starts with a default power, which is set depending on the laser feed rate. In the fourth step, once this initial phase is completed, the algorithm performs the measurement of 2 parameters for each simulation step. On the one hand, the algorithm measures the temperature difference between the hottest node of the solid and the reference temperature initially indicated. In addition, it is also measured at what rate the temperature of the hottest node is increased in two consecutive steps of simulation, that is, at which "speed" is increasing the temperature of the hottest node, which can give an idea of what is the thermal inertia in the solid. Finally, in the fifth step, with these two measured parameters, the error with respect to the Tref and the rate of variation of temperature in the target area ("Taux") between two consecutive steps, 6 different criteria come into play, which manage the delivered power for each of the possible situations. Taux temperature is calculated as the mean temperature in the joining area. In particular, these 6 criteria depend on the error at the reference temperature, and are classified as it is shown in Table 3. Each criteria in Table 3 takes into account two values, the difference between Tref and Taux and the variation of the maximum temperature Tmax in two previous steps. Depending on these values, the power input is adjusted in each simulation step making it a fraction of the initial reference power ("Pot_inicial") or adjusting its value relatively to its value in a previous step ("Pot_mod").

Table 3. Power control criteria

| | 1st Value | 2nd Value | Power Set |
|------------|---------------------|-----------------------------|------------------------|
| Criteria 1 | Tref-Taux>200K | | Pot_mod= Pot_inicial/3 |
| | | Tmax(t-1)-Tmax(t-2)<3K | Pot_mod=Pot_modx1.2 |
| Criteria 2 | 200>Tref-Taux>50K | 3K<Tmax(t-1)-Tmax(t-2)<30K | Pot_mod=Pot_inicial/3 |
| | | Tmax(t-1)-Tmax(t-2)>30K | Pot_mod=Pot_modx0.95 |
| Criteria 3 | 50>Tref-Taux>10K | Tmax(t-1)-Tmax(t-2)<4K | Pot_mod=Pot_modx1.2 |
| | | 4K<Tmax(t-1)-Tmax(t-2)<15K | Pot_mod=Pot_inicial/6 |
| | | Tmax(t-1)-Tmax(t-2)>15K | Pot_mod=Pot_modx0.95 |
| Criteria 4 | 10>Tref-Taux>-10K | Tmax(t-1)-Tmax(t-2)<1.5K | Pot_mod=Pot_modx1.2 |
| | | 1.5K<Tmax(t-1)-Tmax(t-2)<5K | Pot_mod=Pot_inicial/6 |
| | | Tmax(t-1)-Tmax(t-2)>5K | Pot_mod=Pot_modx0.95 |
| Criteria 5 | -10K>Tref-Taux>-60K | | Pot_mod=Pot_modx0.80 |
| Criteria 6 | Tref-Taux<-60K | | Pot_mod=Pot_modx0.7 |

3.2 Power control system result discussion

Several simulation were carried out in order to test the performance of the power control system. Sample parts of 100x25x2mm were simulated. A regular mesh with 10,000 nodes was programmed. The laser used in this simulations was a diode laser guided by optical fiber and with a spot of 10mm in diameter. In a first approach a simulation of temperature field without power control was carried out. Materials simulated were AISI 304 Stainless Steel and Texpex 102. The TEPEX was simulated as boundary condition of the joining interface on stainless steel to adjust the thermal conductivity. The laser input was on the opposite face to the joining. In the first simulation, without power control system, rectangular trajectory of 8x18mm was simulated. The first point of the trajectory was located at 4mm from X and Y axis, then, trajectory parallel to Y axis and X axis was followed with laser beam completing 8x18mm rectangle. The process motion was simulated with feed rate of 50mm/s and constant power input of 850W. In Figure 6 it is shown the temperature evolution in the center point of the 18x8mm rectangle.

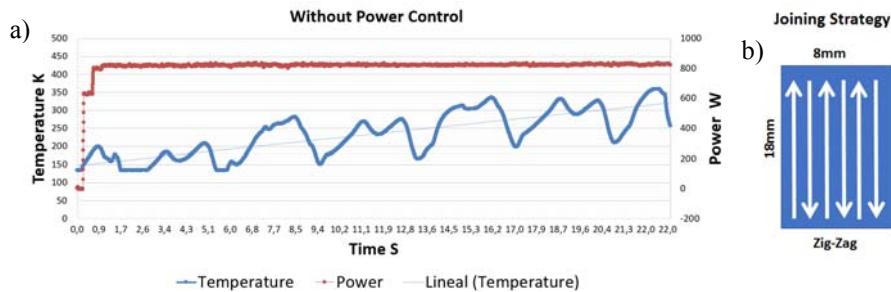


Fig. 5. a) Maximum temperature evolution without power control and b) simulated joining strategies

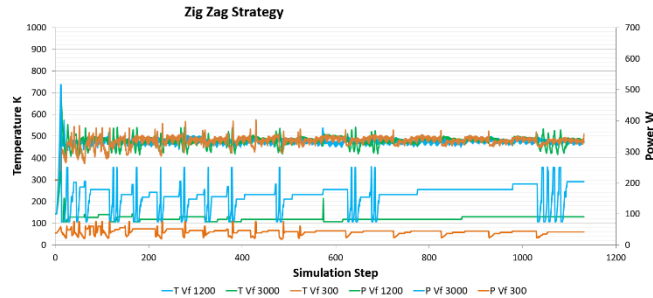


Fig. 6. Zigzag strategy both with power control

Figure 5 a) shows the evolution of temperature with progressive increase instead of reaching a stable temperature. The thermal field, and therefore temperature, is changing in cycles due to the motion of the laser spot and is not possible to reach a uniform thermal field needed for successful joining. In following tests several strategies were simulated with power control activated. Based on previous tests, Zigzag strategy was selected to reach uniform heating (Figure 5b). Same previous 8x18mm area was processed, with same laser spot and with three different feed rates in each strategy. Simulations were carried out for feed rates of 1,200, 300, 3,000 mm/min respectively, so that the adaptability of the algorithm for different speed conditions of the laser could be checked. As mentioned, the reference temperature was set at 500K and the power control algorithm was activated. The geometry used in simulations was the same simulated in the initial test with 25x100x2mm and 10,000 nodes. The result of the simulation was satisfactory, with low fluctuations with respect to the set point and a relatively fast transient as it is shown in Figure 6. With feed rate of 3,000mm/s, the temperature control becomes more difficult and the control system answer generates power variations of 250W in order to compensate thermal field variation due to high feed rate.

4. Conclusions

Successful texturing was reached with CW laser. A controlled material removal rate was obtained with pulses of 100 μ s at 4kHz and 350W. With these parameters dimples of 15 μ m in depth and 100 μ m in diameter were obtained. The overlapping of these dimples allows a controlled material removal and gives as result a surface suitable for dissimilar joining applications. Increasing the number of layers in the texturing process is possible to get different peak-valley structures and adapt them to the melted polymer flow properties. On the other hand, thermal simulation is an effective tool to control the process temperature in the joining interface. A thermal model was programmed in Matlab[®] and original power control system was programmed in order to fix constant the temperature in the joining interface. Several simulations were carried out comparing different scanning feed rates. Initial unstable regime was identified for initial steps when laser beam starts to heat the material. The duration of this instability depends mainly on the strategy, thus, for ZigZag strategy, takes up to 5s to stabilize the thermal field. On the other hand, feed rates between 300 and 1,200mm/s gives satisfactory results with homogeneous temperature and no so aggressive power variations. A feed rate of 3,000mm/s is harder to control and shows to be less accurate when reaching a constant temperature. Finally, an experimental validation will be addressed in future works to validate the new power control algorithm.

Acknowledgements

This work was carried out with the funding help received from PARADDISE project ID723440 under FoF-13 H2020 program

References

- [1] K.W. Jung, Y. Kawahito, M. Takahashi, S. Katayama, *J. of Laser App.* 25 (2013) 32003–6.
- [2] J. Esteves, S. Goushegir, J. Dos Santos, L. Canto, E. Hage, S. Amancio-Filho, *Materials and Design.* 66 (2015) 437–45.
- [3] R. Yeh, R. Hsu., *Int. J. of Adhes. & Adhesives.* 65 (2016) 28–32.
- [4] F. Lambiase, *Int. J. of Adv. Manuf. Techn.* 80 (2015) 1995–2006.
- [5] Z. Huang, S. Sugiyama, J. Yanagimoto, *Proc. Eng.* 81 (2014) 2123–8.
- [6] E. Zhang, J.G. Shan, X.H. Tan, J. Zhang, *Int. J. of Adh. & Adhesives.* 70 (2016) 142–151.
- [7] P. Amend, S. Pfindel, M. Schmidt, *Phys. Proc.* 41 (2013) 98–105.
- [8] F.Y. Sakata, A.M.E. Santo, M. Miyakawa, R. Riva and M.S.F. Lima, *Surf. Eng.* 25 (3) (2009) 180-186.
- [9] D. Weller, J. Simon, P. Stritt, R. Weber, T. Graf, C. Bezençon, C. Bassi, *Phys. Proc.* 83 (2016) 515-522.
- [10] E. Ukar, A. Lamikiz, S. Martinez, I. Arrizubieta, *Proc. Eng.* 132 (2015) 663-670.
- [11] E. Majchrzak, B. Mochnacki, J.S. Suchy, *J. of Theor. and App. Mech.* 47 (2) (2009) 383-396.